Gel–based cell manipulation method for isolation and genotyping of single-adherent cells

Journal:	*Analyst*
Manuscript ID	AN-ART-07-2018-001456.R1
Article Type:	Paper
Date Submitted by the Author:	20-Sep-2018
Complete List of Authors:	Negishi, Ryo; Tokyo University of Agriculture and Technology Iwata, Reito; Tokyo University of Agriculture and Technology Tanaka, Tsuyoshi; Tokyo University of Agriculture + Technology, Department of Biotechnology and Life Science Kisailus, David; University of California Riverside, Chemical and Environmental Engineering; University of California Riverside, Materials Science and Engineering Maeda, Yoshiaki; Tokyo Noko Daigaku Kogakubu Daigakuin Kogaku Kenkyuin Matsunaga, Tadashi; Tokyo University of Agriculture + Technology, Department of Biotechnology Yoshino, Tomoko; Tokyo University of Agriculture and Technology,

Analyst

Gel-based cell manipulation method for isolation and genotyping of single-adherent cells

Ryo Negishi,[a] Reito Iwata,[a] Tsuyoshi Tanaka,[a] David Kisailus,[b] Yoshiaki Maeda,[a] Tadashi Matsunaga,[a, c] and Tomoko Yoshino*[a]

Genetic analysis of single-cells is widely recognized as a powerful tool for understanding cellular heterogeneity and obtaining genetic information from rare populations. Recently, many kinds of single-cell isolation systems have been developed to facilitate single-cell genetic analysis. However, these systems mainly target non-adherent cells or cells in a cell suspension. Thus, it is still challenging to isolate single-adherent cells of interest from a culture dish using a microscope. We had previously developed a single-cell isolation technique termed "gel-based cell manipulation" (GCM). In GCM, single-cells could be visualized by photopolymerizable-hydrogel encapsulation that made it easier to isolate the single-cells. In this study, GCM-based isolation of single-adherent cancer cells from a culture dish was demonstrated. Single-adherent cells were encapsulated in a photopolymerizable hydrogel using a microscope and isolated with high efficiency. Furthermore, whole genome amplification and sequencing for the isolated single-adherent cell could be achieved. We propose that the GCM-based approach demonstrated in this study has the potential for efficient analysis of single-adherent cells at the genetic level.

Introduction

Over the past few years, the use of single-cell analysis has become increasingly valuable over conventional bulk methods to truly understand the properties and dynamic behaviour of individual cells.[1-5] With the emergence of single-cell isolation techniques, there have been significant analytical advances in single-cell omics including genomics, transcriptomics, proteomics, and metabolomics.[6-10] Engineering efforts have been devoted to develop novel techniques to conduct such analyses (e.g., whole genome amplification (WGA), whole transcriptome amplification (WTA), and highly sensitive mass spectrometry). Overcoming these challenges in both single-cell isolation (upstream) and single-cell omics analyses (downstream) might prove to be of great importance to the fields of cell biology, cancer diagnosis, and pharmacology.[11-13]

Fluorescence-activated cell sorting (FACS) is one of the most widely utilized techniques for single-cell isolation.[14, 15] In FACS, individual cells are partitioned into fluidic droplets. Each droplet with a cell is sorted based on the scattering and fluorescence signals obtained from the cell. FACS is a high throughput sorting methodology; however, its drawback is that it requires large number of cells (i.e., approximately 10^5-10^6). Alternatively, microfluidics- and micromanipulation-based isolation systems have been proposed for the analysis of single cells.[13, 16-19] However, the common limitation of these techniques that the single-cells have to be manipulated in their suspended state. These techniques are not suitable for the isolation of the non-suspended cells, which tightly adhere to substrates such as a plastic culture dish.

In contrast to methods for the analysis of suspended cells, development of techniques for the isolation of single-adherent cells has been limited, thus impeding the efforts to analyse the properties of cancer cells and stem cells adhering to a substrate at a single-cell level.[20, 21] Conventional analysis of these cells at a single-cell level use proteolytic enzymes such as trypsin to enable detachment from the substrate. However, this detachment procedure can cause loss of important information (e.g., the position, morphological features, and the neighbouring environment of the cell of interest). For instance, it was reported that morphologies of drug-sensitive and drug-resistant cancer cells adhering on culture dishes were distinguishable.[22] When trypsinized, these cells adapt to a spherical shape in suspension, and becoming indistinguishable. To address this issue, techniques for the direct isolation of single-adherent cells are desired. To date, there are only a few techniques that facilitate the direct isolation of single-adherent cells. However, these approaches require expensive instrumentation, are time consuming, and

[a.] Division of Biotechnology and Life Science, Institute of Engineering, Tokyo University of Agriculture and Technology, 2-24-16, Naka-cho, Koganei, Tokyo, 184-8588, Japan
[b.] Department of Chemical and Environmental Engineering, University of California, Riverside, Room 343 Materials Science and Engineering Building, Riverside, CA 92521, USA
[c.] Waseda Research Institute for Science and Engineering, Waseda University, 3-4-1 Okubo, Shinjuku-ku, Tokyo, 169-8555, Japan

are cumbersome. Therefore, there is a dire need for a less complex approach.

Recently, we developed a simple technique for single-cell isolation, which is termed "gel-based cell manipulation" (GCM)[23]. In GCM, the single-cells are initially recovered, aligned on a microfilter device (termed microcavity array, MCA) based on cell size and deformability.[24, 25] Subsequently, the cells on the MCA are immersed in a photopolymerizable prepolymer, polyethylene glycol diacrylate (PEGDA). Using a fluorescent microscope, the cell of interest is shined by the light at 405 nm, so that PEGDA surrounding the cell can be polymerised. Subsequently the cell is embedded in the PEGDA hydrogel. The diameter of the hydrogel is large enough (~300 μm) to be observed by the naked eye and to be manually manipulated using tweezers. It allows us to isolate single-cells in a simple and efficient way. Single-cell genetic analyses (i.e., DNA analyses) have been performed on single-cells isolated using GCM,[23, 26] but have not yet been applied to adherent cells on a culture dish.

Therefore the focus of this study was to determine if GCM could be used to isolate single-adherent cells. Three types of cancer cells on the culture dish were used for this study. Moreover, the downstream genotyping experiments, including whole genome amplification (WGA) and sequencing, were conducted using the isolated single-adherent cells. According to the results obtained in this study, GCM showed considerable potential for efficient isolation of single-adherent cells.

Experimental

Preparation of cell cultures

Three cell lines, HeLa (cervical cancer cell line), A549 (lung cancer cell line), and NCI-H1975 (lung cancer cell line) were used in this study. The HeLa cell line used in this study was genetically modified from our previous study[27] to express green fluorescent protein (GFP), and thus it was designated as HeLa-GFP. A549 and NCI-H1975 cells were purchased from American type culture collection (ATCC, Manassas, VA, USA). HeLa-GFP cells were cultured in Dulbecco's modified Eagle's medium (DMEM) supplemented with 10% foetal bovine serum (FBS), 1% non-essential amino acids, 2 mM L-glutamine, and 1% penicillin-streptomycin. A549 and NCI-H1975 cells were cultured in RPMI-1650 medium supplemented with 10% FBS and 1% penicillin-streptomycin. Cells were cultured for 3-4 days at 37°C in a humidified atmosphere containing 5% CO_2.

Immediately prior to each experiment, cells grown to approximately 80% confluency were trypsinized and re-suspended in phosphate buffered saline (PBS, pH 7). The cells were stained with 1.6 μM Hoechst 33342 (Thermo Fisher Scientific, Waltham, MA, USA) and 5 μM CellTracker green 5-chloromethylfluorescein diacetate (CMFDA; Thermo Fisher Scientific, Waltham, MA, USA) or 5 μM CellTracker Orange 5-(and-6)-(((4-chloromethyl)benzoyl)amino)tetramethylrhodamine (CMTMR; Thermo Fisher Scientific) for 30 min. The cells were then washed with PBS to remove excess dye. For subsequent GCM steps, a spacer seal (a slide seal for in-situ PCR, inner space: 9 × 9 mm^2, thickness: 300 μm, Thermo Fisher Scientific, Waltham, MA, USA) was affixed at the bottom of a 35 mm culture dish (AGC Techno Glass Co., Ltd, Shizuoka, Japan) prior to addition of the culture medium. After the cell concentration was determined using a microscope and haemocytometer, approximately one thousand tumour cells were suspended in 0.3 mL of the aforementioned media. The cell suspension was then mounted only inside of the inner space of the seal. The cell cultures were incubated at 37°C in a humidified atmosphere containing 5% CO_2 for 24, 48, or 72 h. Subsequently, the medium was removed, and the cells were washed with 1 mL of PBS. The as-prepared cell samples were observed using a fluorescent microscope (BX53; Olympus Co., Tokyo, Japan). Cell adherent area was measured using Image J.[28]

Gel-based cell manipulation (GCM)

Figure 1 illustrates the procedure of GCM for isolation of adherent cells. PEGDA (Mn = 700) prepolymer with 0.5% 1-[4-(2-Hydroxyethoxy)-phenyl]-2-hydroxy-2-methyl-1-propane-1-one (Irgacure 2959) was introduced into the inner space of the spacer seal encompassing the cells. Subsequently, a coverslip was mounted to encase the cells. Coverslips were modified with 3-(trimethoxysilyl)-propyl methacrylate to provide a stiff connection between the coverslip and hydrogel.[29] The subsequent processing steps were similar to the conventional GCM targeting for suspended cells, as described previously.[23] Briefly, light (λ = 365 nm) was focused through the objective lens (UPlanFLN 20X, Olympus Co., Tokyo, Japan) of a fluorescence microscope, and projected onto the cells of interest. Irradiated enargy was measured using a UV power meter C10427 H10428 (Hamamatsu Photonics K.K., Shizuoka, Japan). A hydrogel was solidified by irradiating UV light with the irradiation energy of 12.7 mW/cm^2 for 30 sec. The
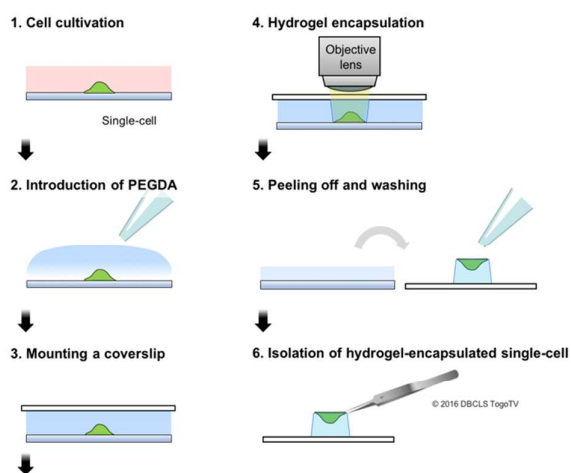

Fig. 1 Schematic illustration of the gel-based cell manipulation (GCM) method for isolation of single-adherent cells.

photopolymerised hydrogels were collected by peeling off of the coverslip. The collected hydrogels were observed using a fluorescence microscope or scanning electron microscope VE-9800 (KEYENCE, Osaka, Japan; after sputter coating a thin layer of gold). The microscope for light irradiation and observation was integrated with a computer-operated motorized stage, WU, NIBA, and WIG filter sets, and a cooled digital camera (Retiga EXi Aqua; QImaging Co., Surrey, BC, Canada). The irradiation intensity of the area was controlled by LuminaVision (Mitani Co., Tokyo, Japan). First, light was irradiated on the hydrogel area without cells. The hydrogel was observed, and the edge of the hydrogel in the field of view was outlined with LuminaVision. The outlined area marked in the field of view was recorded as the irradiated area. Subsequently, the position of the cell(s) of interest was co-adjusted with the irradiation area by moving the stage. When required, mild trypsinization of the cells was performed with 0.03% trypsin/0.0025% EDTA (30 sec), followed by washing by PBS before PEGDA introduction.

We defined that single-cell isolation was successful when both fluorescence of Hoechst 33342 staining nucleus and CellTracker Orange staining cytoplasm were observed in a single-cell on the collected hydrogel. For each cell line, 90 cells (30 cells × 3 dishes) were subjected to GCM. The isolation efficiency was calculated for each dish was as follows:
Isolation efficiency (%) = (number of successful trials of single-cell isolation / 30) × 100.

Fluorescence activated cell sorting (FACS)

Single-cell sorting of suspended HeLa-GFP and NCI-H1975 cells was carried out using FACSAria II (Becton Dickinson, New Jersey, US). The Hoechst 33342- and CellTracker Orange-labelled cells were suspended in PBS and their fluorescence profiles were analysed. The cells were selected based on the intensity of forward scattering and florescence of CellTracker Orange. The cells were sorted into PCR tubes containing 1 µL of PBS.

Whole genome amplification from single-adherent cells

Ampli1 WGA Kit (Silicon Biosystems, Florence, Italy) was used for WGA. First, the hydrogel containing the cells was transferred from the coverslip to a PCR tube using tweezers. Next, WGA was performed by following the manufacture's protocol. The final concentration of the as-prepared WGA products was determined using Quant-iT PicoGreen ds DNA Assay Kit (Thermo Fisher Scientific, Waltham, MA, USA). WGA from the suspended single-cells sorted by FACS was also carried out using the same procedure. The WGA products were purified using a MinElute PCR Purification Kit (Qiagen, Hilden, Germany) by following the manufacturer's protocol. The length of the amplified fragments was analysed using the Agilent DNA 1000 kit (Agilent Biotechnology, Santa Clara, CA, USA).

PCR and sequence analysis

A part of DNA fragment encoding the tumour protein p53 (*TP53*) was amplified by PCR using the purified WGA products as templates with the following forward and reverse primers (exon 8-F, 5'-GGA CAG GTA GGA CCT GAT TT-3'; exon 8-R, 5'-CCA GGA GCC ATT GTC TTT GA-3'). Primers were designed using Primer BLAST. PCR was carried out in 50 µL of PCR mixture containing 1 µL of a WGA product as a template, 0.3 µM each primer, 0.2 mM each dNTP, 5 µL of 10× TaKaRa Ex Taq buffer, and 1.25 U of TaKaRa Ex Taq (TaKaRa Bio Inc., Shiga, Japan) under the following conditions: 3 min at 94°C; followed by 30 cycles of 30 s at 94°C, 10 s at 57°C, and 1 min at 72°C; followed by 2 min at 72°C at the end. Sequence analyses of the amplified fragments were performed with the above primers by Fasmac sequencing service (Kanagawa, Japan) to detect the *TP53* c.818G>A mutation.

Statistics

The data were analysed for significance using Welch's *t*-test. Differences were assessed with a two-side test with an *α* level of 0.05.

Results and discussion

Isolation of single-adherent cells by GCM

We confirmed that the cells cultured on the dishes for 24 h were non-spherical and had extended morphologies, indicating that the cells were adhered to the bottom surface of the dishes (NCI-H1975 cells are shown in Figure 2A. Data for HeLa-GFP and A549 cells are not shown). Irradiation of light on an NCI-H1975 cell (Fig. 2A) resulted in a polymerized hydrogel. We collected the hydrogel after peeling the coverslip. As a result, the intact cell was successfully removed from the culture dish (Fig. 2B). The cells from the light-irradiated area remained on the culture dish (Fig. 2B). The removed cell was transferred to the hydrogel without significant change in shape
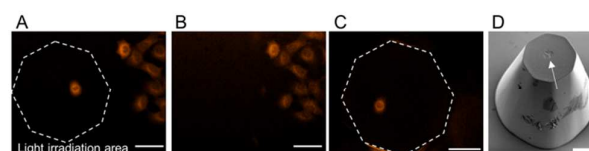

Fig. 2 Microscopic analysis for the isolation of single-adherent cells by GCM. (A) Fluorescence image of the CellTracker Orange-stained NCI-H1975 cells on the culture dish. The white dashed line shows the outlines of the light-irradiated area. (B) Fluorescence image of the remaining cells after removing the hydrogel. (C) Fluorescence image of the cell transferred to the hydrogel. The white dashed line shows the outline of the hydrogel. (D) SEM image of the peeled hydrogel. A single-adherent cell (arrow) was encapsulated at the top surface of the hydrogel. Scale bars: 100 µm

(Fig. 2C). We obtained similar results with HeLa-GFP and A549 cells. These results indicated that GCM facilitated successful isolation of single-adherent cells of the three cell lines. Figure 2D shows an SEM image of a hydrogel containing a NCI-H1975 cell. The three dimensional structure of the hydrogel was shaped like a circular truncated cone on one side, and an octagon on the top surface with the cell (i.e., the bottom surface before peeling the coverslip off) of the hydrogel. The shape of hydrogel was different from that observed in our previous study, in which hydrogel was shaped like a goblet.[23] This could be due to change of light path of excitation light by using objective lens with different magnification.

Next, we compared the isolation efficiency of the three cell lines (HeLa-GFP, A549, and NCI-H1975). As shown in Table 1, isolation efficiencies of HeLa-GFP, A549, and NCI-H1975 were 95.6 ± 3.9%, 95.6 ± 3.9%, and 88.9 ± 9.6%, respectively (data are expressed as mean ± SD of 3 culture dishes, with 30 trials for each dish). The isolation efficiency of NCI-H1975 is lower than those of A549 and HeLa-GFP, although there are no significant differences between NCI-H1975 and A549 or HeLa-GFP (in both cases p = 0.3568, based on Welch's t test). The low isolation efficiency of NCI-H1975 cells might be attributable to a relatively strong adherent force between cell surface and substrate of the culture dish. Besides the physical conditions such as the stiffness of the substrate[30] and temperature,[31] cellular adherent forces are influenced by various factors, including the contact area and intermolecular forces between the cell surface and a substrate (based on interfacial energies), integrin number, and distribution over the cell surface.[32-34] For example, we previously reported that the isolation efficiency of the suspended spherical-shaped NCI-H1975 cells physically entrapped on the nickel-made microcavity arrays was more than 95%,[23] which was higher than that of NCI-H1975 cells adhered on the culture dish (88.9 ± 9.6%). The difference of isolation efficiency could be simply attributed to small contact area between the cell surface and the edge of the microcavity. Therefore, we investigated the relationship between the contact areas and isolation efficiencies of each cell line by measuring the area of the culture dishes covered by the adherent cells (Fig. 3). As per the observations, there was no clear correlation between the distributions of cell areas and isolation efficiencies of any cell line. Despite lower isolation efficiency of NCI-H1975 cells, the distribution of the areas of NCI-H1975 cells were not
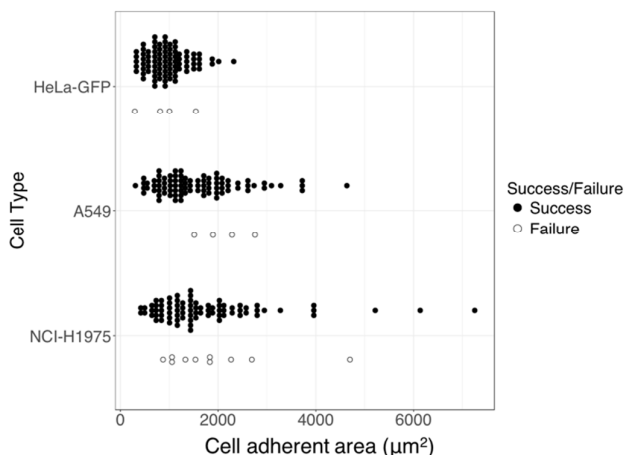

Fig. 3 Evaluation of adhering areas of single cells. Black dots show adhering areas of the cells that were successfully isolated with GCM. White dots represent cells that failed to isolate.

significantly large as compared to those of other two cell lines. From this result, we assumed that NCI-H1975 cells could show a stronger cell adherent force per unit area, resulting in the lower isolation efficiency. Adherent force per unit area can vary depending on the interactions between the cell surface (such as the integrin number) and the substrate (e.g., intermolecular forces). Indeed, the assumption mentioned above is supported by the previous studies reporting that NCI-H1975 cells expressed higher levels of integrin proteins compared to those expressed by A549 and HeLa cells.[35, 36]

If adherent molecules such as integrin are present on the cell surface, they may play key roles to determine the success or failure of cell isolation. Thus, the isolation efficiency should be improved by attenuating these proteins. Based on this assumption, we performed GCM for the cells treated with a low concentration of trypsin (0.03%) for short durations (10 or 30 sec). As predicted, the isolation efficiency was improved by mild trypsinization (Table 1), even though such a benign treatment did not change the shape of adherent cells on culture dish (Fig. S1). This result also supported the idea that isolation efficiency of single-adherent cells by GCM is dependent on the adhesive proteins, like integrin, responsible for cellular adhesion to the substrate.

Table 1 Evaluation of isolation efficiency of single-adherent cell.

		Mild trypsinization	
		10 sec	30 sec
HeLa-GFP	95.6 ± 3.9	98.9 ± 1.9	100.0 ± 0.0
A549	95.6 ± 3.9	97.8 ± 3.9	100.0 ± 0.0
NCI-H1975	88.9 ± 9.6	98.9 ± 1.9	98.9 ± 0.4

Data represent the average isolation efficiency, ± standard deviation. Average isolation efficiency was calculated from three trials. Thirty single-cells were encapsulated for each trial.

ARTICLE

When we compared the areas of the cells that were successfully isolated from the dish and those in the same cell line that failed to be isolated, there was no clear difference (Fig. 3). In other words, some cells with certain cellular areas were successfully isolated, while others of the identical cell line with comparable cell areas were not. Guided by this finding obtained with the aid of GCM-isolated single-adherent cells, we assumed that, even in an identical cell line, individual cells could show different adherent force per unit area. This assumption will be, in part, proved by the analysis of heterogeneity of integrin number and spatial distribution at a single-cell level; however it would be still difficult to do so. Overcoming this difficulty is a challenge that lies ahead.

In addition to considering the cell surface-substrate interactions, cell surface-hydrogel interactions should be considered. It is widely known that cells show little adhesion to unmodified PEG hydrogels although they adhere to the hydrogel modified with the peptides containing an RGD motif[37]. Nonetheless, in the present study, the adherent cells were transferred to hydrogels made of polymerized PEGDA. The underlying mechanism was not fully elucidated and thus further analysis is required in future studies.

Isolation of adherent cells by GCM from dense culture

In the previous section, the single-adherent cells that were spatially segregated from other cells were targeted at each trial. Therefore, there was only a single-cell in the light-irradiated area. However, the final goal is to develop the technique for isolation of arbitral single-adherent cells from confluent cell cultures. Such a technique will be useful for future research, e.g., single-cell isolation from a tissue section.[38, 39] Here, various culture dishes with different cell densities were subjected to GCM. Then, the as-prepared cell cultures were irradiated with light. The number of the cells transferred to the hydrogel with increasing cell density and we found a linear relationship between isolated cell number and light-irradiated cell number (Fig. S2). This result indicated that GCM can recover the adherent cells in dense culture. There is no doubt that, if arbitral single-adherent cells need to be isolated from relatively dense cultures, the light-irradiated area should be limited only to the adherent cells of interest. In the present study, we did not strictly control the area and shape of the surface of the hydrogel in contact with the cells. It was demonstrated that a digital micromirror device (DMD)-based light irradiation system enabled the illumination of a single-cell sized area.[40] Recently, we developed a DMD-based light irradiation system for high throughput single-cell encapsulation.[26] This technology could be a powerful tool for GCM-based single-adherent cell isolation from dense cultures. However, when cells adhere to neighboring cells, intercellular adhesion force needs to be considered. Recent study showed that the intercellular adhesion force was also varied depending on cell type.[41] Thus, for single-cell isolation from confluent culture, we might have to investigate the isolation condition such as mild-trypsinization.

WGA from single-adherent cells isolated by GCM

Beyond demonstrating that GCM enabled the isolation of single-adherent cells with high efficiency, we determined if it was possible to analyse the genotype of the isolated cells. WGA is an essential step for this purpose because the DNA content in a human single-cell is too low (approximately 6 pg per cell) to be analysed. The NCI-H1975 cells and HeLa-GFP cells (10 single-cells for each cell line) were cultured for 24 h, were isolated by GCM, and were subjected to WGA, followed by quantification of the WGA products. Figure 4 summarises the yield of the WGA products of single-adherent cells. For comparison, single-suspended cells prepared by FACS were also used for WGA. The yields of WGA products from HeLa-GFP and NCI-H1975 isolated by GCM were 0.42 ± 0.17 μg and 0.47 ± 0.34 μg, respectively, which were approximately half of those isolated by FACS (0.88 ± 0.46 μg for HeLa-GFP and 0.89 ± 0.50 μg for NCI-H1975; n = 8 for each cell line). The decrease in the WGA yield could be due to multiple factors including the inhibitory effect of cell encapsulation in hydrogel for WGA,[23] leading to the loss or damage of template DNA in the target single-adherent cells (due to the GCM operations). During the GCM operations, the cells adhered to the culture dish were peeled off by breaking potentially strong bonds, such as those from integrin-substrate interactions. We confirmed that this peeling operation did not harm the entire cell structures (Fig. 1); however, we could not completely exclude the possibility that this step can damage the cells on a microscopic level. To decrease potential damage, we trypsinized the cells again, prior to GCM (mild trypsinization for 30 sec). As a result, the WGA yields increased to 1.07 ± 0.46 μg for HeLa-GFP and 1.23 ± 0.10 μg for NCI-H1975 (n = 10 for each cell line), which were
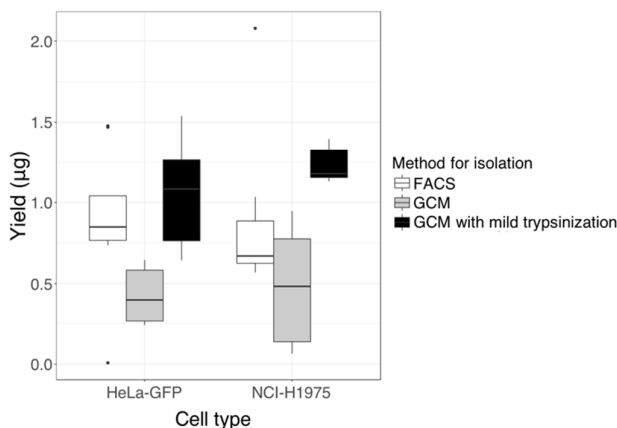

Fig. 4 Evaluation of the yields of whole genome amplification (WGA) products obtained from single-cells. Box plots in white, gray, and black shows the WGA yields of the cells isolated by FACS, by GCM, and GCM with mild trypsinization, respectively.

comparable levels of those of FACS-isolated single-cells. This result suggested that mild trypsinization facilitated isolation of intact single-adherent cells with WGA due to weakening of cell surface-substrate interactions. In this study, we focused on WGA of GCM-isolated single-adherent cells, and whole transcriptome amplification from those will be investigated in the near future. Gene expression analysis of GCM-isolated single-adherent cells will reveal a lot of information including the cellular damages during the isolation process.

Genotyping of single-adherent cells isolated by GCM

Using the WGA products obtained from single-adherent cells, a preliminary genotyping analysis was carried out. It is known that HeLa cells have a wild type *TP53* gene, while NCI-H1975 cells have a mutated one (c.818G>A).[22] We stained these two cell lines by CellTracker Orange, and co-cultured them on a culture dish for 24 h, in order to distinguish these cell lines on the dish using fluorescence microscopy (Fig. 5A). Isolation of the single adherent-cells (n = 8 for each cell line) was carried out by GCM, followed by WGA and PCR using *TP53* specific primers. PCR products were not obtained from 2 samples of NCI-H1975 cells. This could be due to absence of the *TP53* gene in the WGA products caused by the bias during the WGA reaction. Unfortunately, the WGA kits commercially available still have several drawbacks, e.g., poor genetic representation of the entire genome.[42-44] Except for these 2 samples, the mutated *TP53* gene was detected from single-NCI-H1975 cells (n = 6), and the wild type sequence was detected from single-HeLa-GFP cells (n = 8) (Fig. 5B, Fig. S3). This result suggested that GCM has the potential to facilitate the genotypic analysis of single-adherent cells even though the cells with different genotypes were co-cultured on the same dish.

Conclusions

In the present study, we demonstrated that GCM-based approach could be used to isolate single adherent cells. The adherent cells in the light-irradiated area were successfully encapsulated in the PEGDA hydrogel and easily isolated from culture dish with high efficiency. With the aid of mild trypsinization, the isolation efficiency of the single adherent cell and WGA was improved. Furthermore, the isolated cells were also genotyped. These results suggest that GCM has great potential to be used as an effective tool for genetic and morphological characterization of adherent cells at single cell level, which could reveal the underlying cellular heterogeneity.

Conflicts of interest

There are no conflicts to declare.

Acknowledgements

Fig. 5 Genotyping of single-HeLa-GFP cell and single-NCI-H1975 cell isolated from the same culture dish by GCM. (A) Fluorescent image of the co-cultured HeLa-GFP and NCI-H1975 cells on the culture dish. The cells were stained with Hoechst 33342 and CellTracker Orange. Blue and green light (λ = 488 nm and 541 nm, respectively) was used for excitation of GFP and CellTracker Orange. (B) Fluorescent images of the HeLa-GFP and NCI-H1975 cells embedded in the hydrogel. UV light (λ = 365 nm) was used for polymerization of PEGDA prepolymer as well as excitation of Hoechst 33342. GFP and CellTracker Orange were also excited by blue and green light, as described before. The corresponding sequences of the *TP53* gene in a single-HeLa-GFP cell and single-NCI-H1975 cell were analysed by Sanger sequencing. Red triangles represent the position of mutation (c.818G>A) in the NCI-H1975 cells. Scale bars: 50 μm

References

1. P. Van Loo and T. Voet, *Current opinion in genetics & development*, 2014, **24**, 82-91.
2. C. Le Caignec, C. Spits, K. Sermon, M. De Rycke, B. Thienpont, S. Debrock, C. Staessen, Y. Moreau, J. P. Fryns, A. Van Steirteghem, I. Liebaers and J. R. Vermeesch, *Nucleic acids research*, 2006, **34**, e68.
3. K. T. Kim, H. W. Lee, H. O. Lee, S. C. Kim, Y. J. Seo, W. Chung, H. H. Eum, D. H. Nam, J. Kim, K. M. Joo and W. Y. Park, *Genome biology*, 2015, **16**, 127.
4. A. Rotem, O. Ram, N. Shoresh, R. A. Sperling, A. Goren, D. A. Weitz and B. E. Bernstein, *Nature biotechnology*, 2015, **33**, 1165-1172.
5. T. Hayashi, H. Ozaki, Y. Sasagawa, M. Umeda, H. Danno and I. Nikaido, *Nature communications*, 2018, **9**, 619.
6. S. Darmanis, C. J. Gallant, V. D. Marinescu, M. Niklasson, A. Segerman, G. Flamourakis, S. Fredriksson, E. Assarsson, M. Lundberg, S. Nelander, B. Westermark and U. Landegren, *Cell reports*, 2016, **14**, 380-389.
7. D. Ramskold, S. Luo, Y. C. Wang, R. Li, Q. Deng, O. R. Faridani, G. A. Daniels, I. Khrebtukova, J. F. Loring, L. C. Laurent, G. P. Schroth and R. Sandberg, *Nature biotechnology*, 2012, **30**, 777-782.
8. F. Tang, C. Barbacioru, Y. Wang, E. Nordman, C. Lee, N. Xu, X. Wang, J. Bodeau, B. B. Tuch, A. Siddiqui, K. Lao and M. A. Surani, *Nature methods*, 2009, **6**, 377-382.
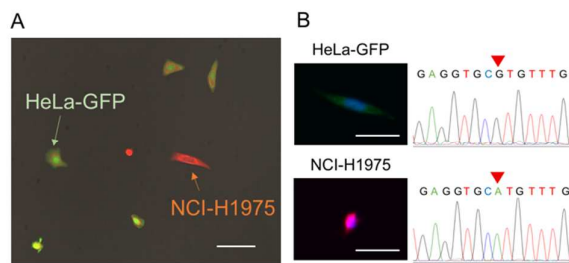
9. C. Chen, D. Xing, L. Tan, H. Li, G. Zhou, L. Huang and X. S. Xie, *Science*, 2017, **356**, 189-194.

10. P. Shahi, S. C. Kim, J. R. Haliburton, Z. J. Gartner and A. R. Abate, *Scientific reports*, 2017, **7**, 44447.

11. B. Spanjaard, B. Hu, N. Mitic, P. Olivares-Chauvet, S. Janjuha, N. Ninov and J. P. Junker, *Nature biotechnology*, 2018, **36**, 469-473.

12. D. T. Miyamoto, Y. Zheng, B. S. Wittner, R. J. Lee, H. Zhu, K. T. Broderick, R. Desai, D. B. Fox, B. W. Brannigan, J. Trautwein, K. S. Arora, N. Desai, D. M. Dahl, L. V. Sequist, M. R. Smith, R. Kapur, C. L. Wu, T. Shioda, S. Ramaswamy, D. T. Ting, M. Toner, S. Maheswaran and D. A. Haber, *Science*, 2015, **349**, 1351-1356.

13. N. Shembekar, C. Chaipan, R. Utharala and C. A. Merten, *Lab on a chip*, 2016, **16**, 1314-1331.

14. M. L. Leung, Y. Wang, C. Kim, R. Gao, J. Jiang, E. Sei and N. E. Navin, *Nature protocols*, 2016, **11**, 214-235.

15. M. Enge, H. E. Arda, M. Mignardi, J. Beausang, R. Bottino, S. K. Kim and S. R. Quake, *Cell*, 2017, **171**, 321-330 e314.

16. F. Fabbri, S. Carloni, W. Zoli, P. Ulivi, G. Gallerani, P. Fici, E. Chiadini, A. Passardi, G. L. Frassineti, A. Ragazzini and D. Amadori, *Cancer letters*, 2013, **335**, 225-231.

17. D. J. Peeters, B. De Laere, G. G. Van den Eynden, S. J. Van Laere, F. Rothe, M. Ignatiadis, A. M. Sieuwerts, D. Lambrechts, A. Rutten, P. A. van Dam, P. Pauwels, M. Peeters, P. B. Vermeulen and L. Y. Dirix, *British journal of cancer*, 2013, **108**, 1358-1367.

18. K. Yamanaka, M. Saito, M. Kita, Y. Takamura, G. Hashiguchi, H. Takabayashi and E. Tamiya, *Sensors and Actuators B: Chemical*, 2013, **178**, 678-682.

19. J. Kim, H. Cho, S. I. Han and K. H. Han, *Analytical chemistry*, 2016, **88**, 4857–4863.

20. M. Valiente, Anna C. Obenauf, X. Jin, Q. Chen, Xiang H. F. Zhang, Derek J. Lee, Jamie E. Chaft, Mark G. Kris, Jason T. Huse, E. Brogi and J. Massagué, *Cell*, 2014, **156**, 1002-1016.

21. N. Akrap, D. Andersson, E. Bom, P. Gregersson, A. Stahlberg and G. Landberg, *Stem Cell Reports*, 2016, **6**, 121-136.

22. B.-X. Zhao, J. Wang, B. O. Song, H. Wei, W.-P. Lv, L.-M. Tian, M. E. I. Li and S. Lv, *Molecular Medicine Reports*, 2015, **11**, 2767-2774.

23. T. Yoshino, T. Tanaka, S. Nakamura, R. Negishi, M. Hosokawa and T. Matsunaga, *Analytical chemistry*, 2016, **88**, 7230-7237.

24. M. Hosokawa, H. Kenmotsu, Y. Koh, T. Yoshino, T. Yoshikawa, T. Naito, T. Takahashi, H. Murakami, Y. Nakamura, A. Tsuya, T. Shukuya, A. Ono, H. Akamatsu, R. Watanabe, S. Ono, K. Mori, H. Kanbara, K. Yamaguchi, T. Tanaka, T. Matsunaga and N. Yamamoto, *PloS one*, 2013, **8**, e67466.

25. M. Hosokawa, T. Hayata, Y. Fukuda, A. Arakaki, T. Yoshino, T. Tanaka and T. Matsunaga, *Analytical chemistry*, 2010, **82**, 6629-6635.

26. R. Negishi, K. Takai, T. Tanaka, T. Matsunaga and T. Yoshino, *Analytical chemistry*, 2018, DOI: 10.1021/acs.analchem.8b00896.

27. F. Saito, H. Yokota, Y. Sudo, Y. Yakabe, H. Takeyama and T. Matsunaga, *Toxicology in Vitro*, 2008, **22**, 1077-1087.

28. C. A. Schneider, W. S. Rasband and K. W. Eliceiri, *Nature methods*, 2012, **9**, 671-675.

29. V. A. Liu and S. N. Bhatia, *Biomedical microdevices*, 2002, **4**, 257-266.

30. T. Yeung, P. C. Georges, L. A. Flanagan, B. Marg, M. Ortiz, M. Funaki, N. Zahir, W. Ming, V. Weaver and P. A. Janmey, *Cell Motil Cytoskeleton*, 2005, **60**, 24-34.

31. F. Rico, C. Chu, M. H. Abdulreda, Y. Qin and V. T. Moy, *Biophysical journal*, 2010, **99**, 1387-1396.

32. D. W. Zhou and A. J. Garcia, *Journal of biomechanical engineering*, 2015, **137**, 020908.

33. N. D. Gallant, K. E. Michael and A. J. Garcia, *Mol Biol Cell*, 2005, **16**, 4329-4340.

34. A. Rizwan, M. Cheng, Z. M. Bhujwalla, B. Krishnamachary, L. Jiang and K. Glunde, *NPJ Breast Cancer*, 2015, **1**, 15017.

35. K. Pyrc, P. Merilahti, S. Tauriainen and P. Susi, *PloS one*, 2016, **11**.

36. A. Babu, N. Amreddy, R. Muralidharan, G. Pathuri, H. Gali, A. Chen, Y. D. Zhao, A. Munshi and R. Ramesh, *Scientific reports*, 2017, **7**.

37. J. A. Burdick and K. S. Anseth, *Biomaterials*, 2002, **23**, 4315-4323.

38. S. Marques, A. Zeisel, S. Codeluppi, D. van Bruggen, A. Mendanha Falcao, L. Xiao, H. Li, M. Haring, H. Hochgerner, R. A. Romanov, D. Gyllborg, A. B. Munoz-Manchado, G. La Manno, P. Lonnerberg, E. M. Floriddia, F. Rezayee, P. Ernfors, E. Arenas, J. Hjerling-Leffler, T. Harkany, W. D. Richardson, S. Linnarsson and G. Castelo-Branco, *Science*, 2016, **352**, 1326-1329.

39. A. Mikulowska-Mennis, T. B. Taylor, P. Vishnu, S. A. Michie, R. Raja, N. Horner and S. T. Kunitake, *Biotechniques*, 2002, **33**, 176-179.

40. M. P. Chien, C. A. Werley, S. L. Farhi and A. E. Cohen, *Chem Sci*, 2015, **6**, 1701-1705.

41. A. Sancho, I. Vandersmissen, S. Craps, A. Luttun and J. Groll, *Scientific reports*, 2017, **7**. 46152.

42. E. Borgstrom, M. Paterlini, J. E. Mold, J. Frisen and J. Lundeberg, *PloS one*, 2017, **12**, e0171566.

43. L. Deleye, L. Tilleman, A. S. Vander Plaetsen, S. Cornelis, D. Deforce and F. Van Nieuwerburgh, *Scientific reports*, 2017, **7**, 3422.

44. E. Normand, S. Qdaisat, W. Bi, C. Shaw, I. Van den Veyver, A. Beaudet and A. Breman, *Prenat Diagn*, 2016, **36**, 823-830.